Published in final edited form as:
Development. 2005 May ; 132(9): 2047–2056.

Ventral migration of early-born neurons requires *Dcc* and is essential for the projections of primary afferents in the spinal cord

Yu-Qiang Ding[1,*], **Ji-Young Kim**[1], **Yong-Sheng Xu**[1], **Yi Rao**[2,†], and **Zhou-Feng Chen**[1,‡]

1*Departments of Anesthesiology, Psychiatry, Molecular Biology and Pharmacology, School of Medicine, Washington University Pain Center, St Louis, MO 63110, USA*

2*Anatomy and Neurobiology, School of Medicine, Washington University Pain Center, St Louis, MO 63110, USA*

Summary

Neuronal migration and lamina-specific primary afferent projections are crucial for establishing spinal cord circuits, but the underlying mechanisms are poorly understood. Here, we report that in mice lacking *Dcc* (deleted in colorectal cancer), some early-born neurons could not migrate ventrally in the spinal cord. Conversely, forced expression of *Dcc* caused ventral migration and prevented dorsolateral migration of late-born spinal neurons. In the superficial layer of the spinal cord of $Dcc^{-/-}$ mutants, mislocalized neurons are followed by proprioceptive afferents, while their presence repels nociceptive afferents through *Sema3a*. Thus, our study has shown that *Dcc* is a key molecule required for ventral migration of early-born neurons, and that appropriate neuronal migration is a prerequisite for, and coupled to, normal projections of primary afferents in the developing spinal cord.

Keywords

Dcc; Early-born neuron; Migration; Primary afferents; Spinal cord; Mouse

Introduction

In the developing dorsal spinal cord, different classes of postmitotic neurons, once emerging from the ventricular zone (VZ), migrate with remarkable precision. Two waves of neuronal migration have been found recently, both originating from the VZ: neurons born prior to E11.5 (early-born neurons) predominantly migrate ventrally or ventrolaterally, whereas neurons born afterwards (late-born neurons) migrate along dorsolateral direction and form the dorsal horn (Caspary and Anderson, 2003; Helms and Johnson, 2003). Six classes of early-born dorsal interneurons (dI1-6) are classified according to their unique gene expression profile. These neurons show distinct migration pattern: dI1-3 neurons appear to migrate ventrally along the midline region, whereas dI4-6 neurons follow ventrolateral routes (Gross et al., 2002; Muller et al., 2002; Qian et al., 2002; Saba et al., 2003). Many of early-born neurons are commissural neurons and migrate to the intermediate region of the spinal cord. What promotes early-born neurons to migrate along the dorsoventral pathways is not clear.

‡Author for correspondence (e-mail: chenz@wustl.edu).
*Present address: Laboratory of Neural Development, Institute of Neuroscience, Chinese Academy of Sciences, 320 Yue Yang Road, Shanghai, 200031, PR China
†Present address: Department of Neurology, Northwestern University Feinberg School of Medicine, 303 E Chicago Avenue, Ward 10-185, Chicago, IL 60611, USA

Supplementary material for this article is available at http://dev.biologists.org/cgi/content/full/132/9/2047/DC1

Another major event concurring is the projection of different classes of primary sensory afferents within the spinal cord (Brown, 1981; Ozaki and Snider, 1997). The projections of distinct classes of primary afferents differ not only in their final termination sites but also in their entry routes in the dorsal horn. For example, proprioceptive afferents enter the spinal cord through the medial region, whereas nociceptive afferents innervate laminae I-II of the dorsal horn through the lateral region (Brown, 1981; Ozaki and Snider, 1997) (Fig. 1A). In mice, the ETS transcription factor *ER81* and a Runx transcription factor *Runx3* are required in the dorsal root ganglion (DRG) for the projection of proprioceptive afferents in the spinal cord (Arber et al., 2000; Inoue et al., 2002; Patel et al., 2003). Peripheral signaling such as NT3 is also important for the central patterning of proprioceptive afferents (Lin et al., 1998; Patel et al., 2003). In addition, central target-derived signals are required as well for primary afferent projection. For example, the transcription factor *Lmx1b* is required specifically in the dorsal horn for the projection of cutaneous afferents (Ding et al., 2004). Among axonal guidance molecules, *Sema3a* is one of the most intensively studied molecules in the spinal cord, and may play a role in repelling the projections of primary afferents (He and Tessier-Lavigne, 1997; Kolodkin et al., 1997). Although the factors controlling the projections of primary afferents are beginning to be understood, much less is known about the relationship between neuronal migration and precise primary afferent projections during spinal cord development.

Dcc, a transmembrane protein of the immunoglobulin superfamily, is a receptor for axonal guidance molecule netrin 1 (Ntn1) (Fearon et al., 1990; Keino-Masu et al., 1996). In the developing spinal cord, *Dcc* is important for the outgrowth of ventral commissural axons (Fazeli et al., 1997). *Dcc* and its homolog have also been implicated in the migration of several types of cells in different tissues or organisms such as *C. elegans* (Chan et al., 1996; Murase and Horwitz, 2002; Schwarting et al., 2001).

In this study, we have used both loss- and gain-of-function approaches to address mechanisms underlying neuronal migration and primary afferent projections. We found that *Dcc* is both necessary and sufficient for directing the migration of developing spinal neurons towards the ventral spinal cord. Moreover, we showed that early-born neurons can repel nociceptive primary afferents through the activity of *Sema3a* in the developing spinal cord.

Materials and methods

Genotyping and maintenance of animals

$Dcc^{+/-}$ and $Dcc^{-/-}$ mutant mice were genotyped as previously described (Fazeli et al., 1997). To visualize $Math1^{+}$ dI1 neurons in the $Dcc^{-/-}$ mutant by X-gal staining, we crossed $Dcc^{+/-}$ mice with $Math1^{+/-}$ mice (Bermingham et al., 2001). The morning that vaginal plugs were observed was considered to be E0.5. For each set of experiments, at least four $Dcc^{-/-}$ mutant and five wild-type mice were used. *Unc5h3* (*Unc5c* – Mouse Genome Informatics) mutant mice were obtained from The Jackson Laboratory. $Dcc^{-/-}$ mutant mice and *Unc5h3* mutant mice were maintained in a mouse facility, according to protocols approved by the Division of Comparative Medicine at Washington University School of Medicine.

BrdU labeling and detection by immunocytochemistry

Pregnant female mice derived from timed matings between wild-type mice or $Dcc^{+/-}$ mice were given a single intraperitoneal injection of BrdU (5 mg/ml solution in PBS and 60 μg/g of body weight) on 10.5 days postcoitum (dpc), 11.5 dpc and 12.5 dpc. After time periods of 1 day, 2 days, 3 days or 4 days, embryos were removed, genotyped and sectioned as described (Chen et al., 1998a; Chen et al., 2001; Roberts et al., 1994). The sections were stained sequentially with mouse antibody against BrdU (Molecular Probes; 1:200), biotin-conjugated donkey anti-mouse IgG (Jackson Immuno; 1:200), and Cy3-labeled streptavidin (Jackson

Immuno; 1:1000) or *Elite* ABC kit (Vector; 1:200). For anti-BrdU antibody detection, a nickel intensification technique was used. To quantify the distribution of E10.5 BrdU-labeled neurons, Photoshop (Adobe) program was used to divide the spinal cord into dorsal and ventral halves by the sulcus limitans. BrdU-labeled neurons in the two halves were counted in ten sections from four wild-type mice for each group.

Nissl staining, X-gal staining, in situ hybridization and immunocytochemistry

Nissl staining, X-gal staining, in situ hybridization and immunocytochemistry were performed as described (Chen et al., 1998b; Chen et al., 2001; Wang et al., 1998). Briefly, embryos were fixed with 4% paraformaldehyde overnight at 4°C, cryoprotected with 15% sucrose, and sectioned at a thickness of 12 μm. For X-gal staining, the sections were incubated in X-gal buffer (5 mM potassium ferrocyanide, 5 mM potassium ferricyanide, 0.2% Triton X-100, 1 mM $MgCl_2$ and 1 mg/ml X-gal in PBS). For immunocytochemistry, the following antibodies were used: guinea pig (Gp) anti-*Isl1* (gift from T. Jessell; 1:4000), Gp anti-*Lmx1b* (gift from T. Jessel; 1:4000), rabbit anti-*Math1* (gift from J. Johnson; 1:500), rabbit anti-TrkA (gift from L. Recharidt; 1:4000), rabbit anti-*Phox2a* (gift from J. Brunet; 1:4000), rabbit anti-*Pax2* (Zymed Lab; 1:400), mouse anti-2H3 (DSHB; 1:50), goat anti-*Dcc* (Santa Cruz; 1:200), rabbit anti-Peripherin 57K (Chemicon; 1:2000), rabbit anti-Calbindin 28K (Chemicon;. 1:2000) and mouse anti-Parvalbumin (Chemicon; 1:2000). For in situ hybridization, the hybridization signals were visualized upon nitro blue tetrazolium chloride and 5-bromo-4-chloro-3-indolyl phosphate staining.

DiI labeling

DiI labeling was performed as previously described (Ding et al., 2004). Briefly, to label the projection of DRG axons to the spinal cord, DiI crystals (Molecular Probes) were placed in the DRG. The tissues were kept in 4% paraformaldehyde at 37°C for 2-6 days before they were sectioned on a vibratome at a thickness of 50-100 μm. Labeling was observed with epifluorescent or laser confocal microscopy.

In utero electroporation of *Dcc* and *Sema3a*

In utero electroporation was performed according to previous procedures (Saito and Nakatsuji, 2001). Briefly, pregnant wild-type mice at 12.5 dpc were anesthetized with sodium pentobarbital (40 mg/kg), followed by the exposure of the uterus and cutting of the uterine wall on both horns along the antiplacental side. A mixture of pCAGGS-*Dcc* or pCAGGS-*Sema3a* with pCAGGS-EGFP (Niwa et al., 1991) (2 μl; 1 μg/μl for each vector) was injected into the central canal of the spinal cord. PCAGGS-EGFP was injected into different embryos and they were served as control. After the injection, square electric pulses were delivered by the use of an Electro Square Porator (ECM830) at a rate of one pulse per second (voltage 25 V, 5 pulses, 50 ms pulses) to embryos by holding the yolk sac with forceps-type electrodes. Expression of electroporated exogenous genes was examined by in situ hybridization and immunohistochemistry as described above. For counting electroporated cells (EGFP/*Dcc* and EGFP only) in the spinal cord, 7-10 sections from each embryo were counted (four embryos for EGFP and seven embryos for EGFP/*Dcc*).

Quantification of $TrkA^+$ fibers in the dorsal horn of *Sema3a* electroporated spinal cord

The areas of TrkA-positive staining were quantified by the use of software (MetaMorph, 6.2; Universal Imaging Corporation, Downingtown, PA, USA) and a comparison between the electroporated and contralateral sides was performed using Student's *t*-test. Intensity of a pixel above 110 was considered to be positive and areas of TrkA-positive fibers were measured by the software. Areas are indicated in μm^2. Twenty-five images from five electroporated embryos were used for the quantification.

Results

Early-born neurons do not contribute to the formation of the superficial dorsal horn of the spinal cord

To further examine two waves of neuronal migration in the developing dorsal spinal cord, we carried out BrdU labeling experiment in mice. BrdU was first injected into 10.5 dpc pregnant mice, and the distribution patterns of $BrdU^+$ neurons in the spinal cord were examined at E11.5, E12.5 and E13.5 by immunocytochemical staining. At E11.5 and E12.5, numerous $BrdU^+$ cells were found in the dorsal part of the spinal cord (Fig. 1B; data not shown). At E13.5, while $BrdU^+$ cells were found in the intermediate region and ventral horn, no $BrdU^+$ cells were found in the superficial layer of the dorsal spinal cord (Fig. 1C). No significant cell death was found in the spinal cord of BrdU-injected embryos by TUNEL studies (data not shown). Cell counting indicated that about 76% of $BrdU^+$ cells were found in the dorsal half of the neural tube at E11.5 (Fig. 1D). At E12.5, the number of $BrdU^+$ cells was decreased in the dorsal half, but increased in the ventral half of the spinal cord accordingly (Fig. 1D). At E13.5, the number of $BrdU^+$ cells in the dorsal half of the spinal cord was further significantly reduced to less than 10%, whereas the number of $BrdU^+$ cells has markedly increased in the ventral half of the spinal cord (Fig. 1D). Because the total numbers of $BrdU^+$ cells were similar from E11.5 to E13.5, the changes in the distribution of the cells in different regions indicate that these cells were migrating from the dorsal part to the ventral part from E11.5 to E13.5.

By contrast, when BrdU was injected at E11.5, $BrdU^+$ cells were found in the dorsal horn of the spinal cord at E13.5 (Fig. 1E). Similarly, when BrdU was injected at E12.5, $BrdU^+$ cells were also found in the dorsal horn at E14.5 (Fig. 1F). Taken together, our study demonstrates that early-born neurons (born prior to E11.5) migrate ventrally, and do not contribute to the formation of the superficial layer of the dorsal spinal cord. The superficial dorsal horn neurons comprise only those born at E11.5 or afterwards. Although these results are in consistent with previous molecular marker studies (Gross et al., 2002), we, for the first time, clearly demonstrate that early-born neurons do not contribute to the formation of the superficial dorsal horn of the spinal cord.

Dcc is expressed in early-born neurons of the spinal cord

To study the molecular basis for the control of ventral migration of early-born neurons, we have examined expression of *Dcc* in the spinal cord. *Dcc* was most abundantly expressed in the region lining along the VZ of the neural tube between E10.5 and E11.5 (Fig. 2A). *Dcc* was not detected in DRG neurons. In the developing neural tube, *Dcc* is expressed in dI1-2 neurons (Helms and Johnson, 1998) (Fig. 2A,B). Double immunocytochemical staining of *Dcc* and *Isl1* (dI3 marker) showed that *Dcc* was also colocalized with *Isl1*, except in a few $Isl1^+$ neurons (Lee and Jessell, 1999) (Fig. 2B,C). *Isl1* staining was detected in the nuclei, while *Dcc* expression was enriched in the axons and membranes (Fig. 2C). In addition, *Dcc* was co-expressed with *Lmx1b* (dI5 marker) (Fig. 2D,E), and *Pax2* (dI4 and dI6 marker) (Fig. 2F-H) (Burrill et al., 1997;Chen et al., 2001). At E12.5, *Dcc* was detected in the dorsal side of the spinal cord, probably in the migrating early-born neurons (see Fig. S1A in the supplementary material). At E13.5 and E14.5, *Dcc* was not detected in the superficial dorsal horn of the spinal cord where late-born neurons were present (see Fig. S1B,C in the supplementary material). Thus, *Dcc* is expressed in all classes of early-born dorsal interneurons, but not in late-born neurons.

Impaired ventral migration of early-born cells in *Dcc* mutant mice

To assess the role of *Dcc* in the developing dorsal spinal cord, we first examined the morphology of the dorsal spinal cord of *Dcc* mutants by Nissl staining. At E14.5, late-born neurons populated in the dorsal horn became condensed into distinct laminae (Fig. 3A). The

presumptive laminae I-II (superficial dorsal horn) contained numerous darkly stained small neurons that differ from those located in deeper laminae (Fig. 3A). In *Dcc*$^{-/-}$ mutants, however, homogenous distribution of the presumptive laminae I-II cells was disrupted in the medial superficial dorsal horn (Fig. 3B). A cohort of lightly stained cells (distinct from darkly stained cells) was present in the medial laminae I-II (Fig. 3B). To determine whether the lightly stained cells were laminae I-II neurons, *Lmx1b* expression was examined (Chen et al., 2001). In contrast to wild-type control, in which *Lmx1b*$^{+}$ neurons were evenly distributed in laminae I-II (Fig. 3C), a small area corresponding to the position of lightly stained cells was completely devoid of *Lmx1b*$^{+}$ neurons (Fig. 3D).

To determine whether lightly stained/*Lmx1b*-negative cells in laminae I-II were early-born neurons, we examined *Math1* (dI1 marker) expression in *Dcc*$^{-/-}$/*Math1*$^{+/-}$ mice (Bermingham et al., 2001). Because the *lacZ* gene was introduced into the *Math1* locus, we were able to follow *Math1*$^{+}$ cells in *Dcc*$^{-/-}$ mutants at later stages by X-gal staining (Bermingham et al., 2001). In E14.5 *Math1*$^{+/-}$ embryos, *Math1*$^{+}$ cells were present in the intermediate region and were not found in the superficial dorsal horn (Fig. 3E). By contrast, though there were *Math1*$^{+}$ cells in their normal position, some were found ectopically in the medial superficial dorsal horn of *Dcc*$^{-/-}$ mutants (Fig. 3F). Examination of *Isl1* (dI3 marker) in E14.5 wild-type and *Dcc*$^{-/-}$ mutants showed some of *Isl1*$^{+}$ neurons that should have migrated to the intermediate region in the wild-type had stayed in the dorsal part (Fig. 3G,H).

To rule out the possibility that the ectopic presence of *Isl1*$^{+}$ and *Math1*$^{+}$ cells was due to a cell fate switch from late-born neurons to early-born ones, BrdU was injected into 10.5 dpc pregnant mice. At this stage, cells incorporating BrdU should be early-born neurons in the dorsal neural tube. Unlike wild-type embryos, whose early-born neurons labeled by BrdU had settled in the intermediate region and ventral horn, but were not present in the superficial dorsal horn by E14.5 (Fig. 3I), a cohort of BrdU^{+} cells was detected in the medial superficial dorsal horn of *Dcc*$^{-/-}$ mutants (Fig. 3J). When the spinal cord of *Dcc*$^{-/-}$ mutants labeled with BrdU at E11.5 was examined at E14.5, an area was devoid of BrdU^{+} cells in the medial part of laminae I-II of *Dcc*$^{-/-}$ mutants (Fig. 3L), which was different from wild-type embryos whose superficial layer comprised evenly distributed BrdU^{+} cells (Fig. 3K). These results suggest that many of early-born cells aberrantly migrated to the medial superficial dorsal horn and failed to migrate ventrally in *Dcc*$^{-/-}$ mutants.

We next sought to determine whether the migration of all classes or only subsets of early-born neurons were impaired and how early the defects might have occurred in *Dcc*$^{-/-}$ mutants. At E10.5, a stream of *Math1*$^{+}$ cells were lining the dorsal-most VZ, suggesting that *Math1*$^{+}$ cells migrated to their destination (Fig. 4A). However, *Dcc*$^{-/-}$ mutant *Math1*$^{+}$ cells remained in the region adjacent to the roof plate and few *Math1*$^{+}$ cells were found at more ventral regions of the dorsal neural tube (Fig. 4B). Examination of *FoxD3* (dI2 marker) expression showed a defect similar to *Math1* staining pattern in *Dcc*$^{-/-}$ mutants at E10.5 (Fig. 4C,D) (Gross et al., 2002). Although no apparent defect was found in *Isl1* staining pattern at E10.5, more *Isl1*$^{+}$ cells were accumulated in the dorsal aspect of the neural tube of *Dcc*$^{-/-}$ mutant compared with the control at E11.5 (Fig. 4E,F). Double staining of *Pax2* (dI4 and dI6 marker) and *Lmx1b* (dI5 marker) also revealed an aberrant distribution of *Lmx1b*$^{+}$ cells in *Dcc*$^{-/-}$ mutants (Fig. 4G,H). A few *Lmx1b*$^{+}$ cells were found in more dorsal regions of the neural tube. This result was further confirmed by *Phox2a* (dI5 marker) staining in *Dcc*$^{-/-}$ mutant embryos (Ding et al., 2004). A few *Phox2a*$^{+}$ cells appeared to have migrated aberrantly along the dorsal direction (Fig. 4I,J). In addition, there was no change in numbers of cells labeled by each markers examined between wild-type and *Dcc*$^{-/-}$ mutant mice. Taken together, our results indicate that a majority of early-born cells depend on *Dcc*-mediated signaling pathway for their ventral migration.

The lack of migration defect in some early-born neurons in *Dcc*$^{-/-}$ mutants prompted us to examine the mutants lacking other receptors for *Ntn1*. For example, *Unc5h3* is another receptor for *Ntn1* and it plays important roles in the neuronal migration in the developing nervous system (Ackerman and Knowles, 1998; Finger et al., 2002). Analysis of *Unc5h3* mutant mice by Nissl and antibody staining revealed a disruption of superficial laminar organization in the medial superficial layer of the dorsal spinal cord (see Fig. S2 in the supplementary material). This defect is reminiscent of the abnormalities found in the dorsal spinal cord of *Dcc*$^{-/-}$ mutants, suggesting that *Unc5h3* may also be required for the migration of a subset of early-born neurons in the dorsal spinal cord.

Dcc promotes ventral migration and prevents dorsolateral migration of late-born neurons

To test whether *Dcc* controls the migratory behavior of spinal cord neurons directly, we introduced *Dcc* expression vectors into the mouse dorsal spinal cord by in utero electroporation (Saito and Nakatsuji, 2001). *Dcc*- and *Egfp*-expressing vectors were electroporated into the spinal cords of E12.5 mouse embryos and the migratory behavior of electroporated neurons was examined at E14.5. In four control embryos that received EGFP only, EGFP^{+} cells were detected predominantly in the electroporated dorsal horn and few EGFP^{+} cells were found in the ventral horn of the spinal cord at E14.5 (Fig. 5A,C). A few EGFP^{+} cells were present in the intermediate region surrounding the central canal of the spinal cord (Fig. 5A). Notably, EGFP^{+} cells were present in laminae I-II (Fig. 5C). Strikingly, in the spinal cord that expressed *Dcc* and *Egfp*, some EGFP^{+} cells were found in the ventral horn of the spinal cord (Fig. 5B). Moreover, EGFP^{+} cells were hardly detected in laminae I-II (Fig. 5D). Double-staining of *Egfp* and *Dcc* indicated that *Dcc* and *Egfp* were colocalized in electroporated cells (Fig. 5E-G). Quantitative analysis indicated that there was no significant difference between the number of EGFP^{+} cells and *Egfp*/*Dcc*$^{+}$ cells in electroporated spinal cords (Fig. 5I). However, the number of EGFP/DCC^{+} cells was markedly increased in the ventral horn and decreased in laminae I-II of electroporated spinal cords compared with the spinal cords electroporated with EGFP only (Fig. 5I,J). We observed this phenotype in five of seven electroporated embryos. Taken together, our results indicate that *Dcc* affects the migration of late-born neurons by promoting their ventral migration and preventing their dorsolateral migration, suggesting that expression of *Dcc* is sufficient to re-direct the migration of late-born neurons, which do not normally express *Dcc*.

Impaired projection of proprioceptive afferents in *Dcc*$^{-/-}$ mutants

To examine whether the projection of proprioceptive afferents was affected in *Dcc*$^{-/-}$ mutants, we performed immunocytochemistry using anti-2H3 antibody that recognized neurofilaments (Dodd et al., 1988). In E14.5 wild-type embryo, proprioceptive afferents labeled by 2H3 staining had reached the intermediate region of the spinal cord and begun to grow toward the motoneurons in the ventral horn (Fig. 6A). By contrast, proprioceptive afferents were barely detected along the midline region in *Dcc*$^{-/-}$ mutants (Fig. 6B). Strikingly, 2H3^{+} afferents terminated aberrantly within laminae I-II (Fig. 6A,B), and appeared to follow ectopic early-born neurons revealed by *Isl1*$^{+}$ staining in wild-type and *Dcc*$^{-/-}$ mutants (Fig. 6C,D). The abnormal location of early-born neurons and aberrant projection of proprioceptive afferents were also detected in the superficial layer of the dorsal horn of *Dcc*$^{-/-}$ mutants at E16.5, E18.5 and P0 (Fig. 7; data not shown). At E18.5, unlike wild-type control, proprioceptive afferents marked by 2H3 staining were aberrantly present in the region that was devoid of both *Lmx1b* and TrkA (Ntrk1 – Mouse Genome Informatics) staining in the superficial dorsal horn of *Dcc*$^{-/-}$ embryo (Fig. 7A-F) (Ding et al., 2004; Huang et al., 1999). At E15.5 and E16.5, DiI labeling experiment further revealed that, in contrast to the control embryo, where proprioceptive afferents growing towards the ventral horn were clearly detected, no DiI-labeled proprioceptive afferents was detected around the intermediate region of the spinal cord in *Dcc*$^{-/-}$ mutants (Fig. 6E,F; data not shown). By E18.5, DiI labeling indicated that although

proprioceptive afferents have reached the ventral horn of the spinal cord of *Dcc*$^{-/-}$ mutants, in contrast to the control, the labeling intensity was reduced markedly (Fig. 7G,H). Some presumptive proprioceptive afferents projected toward the midline region in the intermediate region of the spinal cord (Fig. 7G,H). Similarly, proprioceptive afferents also aberrantly projected to the superficially dorsal horn in the dorsal horn of *Unc5h3* mutant mice (Fig. S2 in the supplementary material). However, despite aberrant entry of proprioceptive afferents, they could reach the ventral horn of the spinal cord of the mutants at E15.5 (Fig. S3 in the supplementary material).

Early-born neurons repels TrkA afferents through *Sema3a*

We next examined whether the ectopic early-born neurons in the superficial dorsal horn of *Dcc*$^{-/-}$ mutants would affect the projection of nociceptive afferents. The nociceptive afferents were revealed by TrkA immunostaining. In E14.5, E18.5 and P0 wild-type embryos, TrkA^{+} afferents were largely confined to laminae I-II of the dorsal horn (Fig. 8A). In *Dcc*$^{-/-}$ mutants, however, there was an area devoid of TrkA^{+} afferents within laminae I-II (Fig. 8B). An adjacent section stained with Nissl indicated that this area exhibited distinct morphological characteristics from other parts of laminae I-II, as mentioned before. One likely explanation is that early-born neurons may secret a chemorepellent to repel the innervation of TrkA^{+} primary afferents. To identify the chemorepellent, we examined the expression of *Sema3a* in the spinal cord of *Dcc*$^{-/-}$ mutant, because *Sema3a* has been shown to be able to repel cutaneous afferents that express TrkA (Luo et al., 1993;Messersmith et al., 1995). In wild-type embryos, *Sema3a* expression was restricted to the intermediate and ventral regions of the spinal cord (data not shown) and was absent in the dorsal horn (Fig. 8C). In *Dcc*$^{-/-}$ mutants, however, a cluster of *Sema3a*$^{+}$ neurons that were presumably early-born neurons were found in the medial superficial dorsal horn (Fig. 8D). To examine whether *Sema3a* affected TrkA^{+} afferent projection, we expressed *Sema3a* and EGFP in the dorsal horn of mouse spinal cord by in utero electroporation (Fig. 8E,F). On the electroporated side of the spinal cord where *Sema3a* and EGFP were detected, the collaterals of TrkA^{+} afferents were much smaller than that on the contralateral side of the spinal cord despite the fact that no abnormal morphology of the dorsal horn was found after electroporation (Fig. 8G,H; data not shown). Quantitative analysis of *TrkA*$^{+}$ areas in the dorsal horn showed a significant difference between the electroporated and contralateral sides of the spinal cord (Fig. 8I). In situ hybridization confirmed that *Sema3a* expression was abundant in the dorsal horn of the electroporated side of the spinal cord (Fig. 8F). In contrast to TrkA^{+} afferent projection, projection of proprioceptive afferent on the electroporated side of the spinal cord appeared normal (data not shown). Thus, these results suggest that early-born neurons repel the ingrowth of TrkA^{+} afferents via *Sema3a*.

Discussion

Molecular marker analysis indicated that migration of the dorsal neurons is temporally regulated in the developing spinal cord: in contrast to neurons born at E11.5 or afterwards, neurons born prior to E11.5 in the dorsal neural tube make minimal contributions to the formation of the dorsal horn (Gross et al., 2002; Muller et al., 2002; Qian et al., 2002). Nevertheless, the issue of whether early-born neurons ever contribute to the superficial dorsal horn remained unsolved because using molecular markers to trace cell migration was complicated by the possibility that gene expression may change in migrating neurons. Using BrdU labeling, we demonstrate that neurons born prior to E11.5 do not contribute to the formation of the superficial dorsal horn. Consistent with previous studies (Gross et al., 2002; Lee et al., 2000; Lee et al., 1998; Muller et al., 2002; Qian et al., 2002), we find that these early-born neurons undergo ventral migration and contribute to the formation of the intermediate region of the spinal cord (Fig. 1). Using both loss- and gain-of-function studies, we provide evidence that *Dcc* is required for ventral migration of early-born neurons, and can

re-direct the migration of late-born neurons, indicating that *Dcc* is both necessary and sufficient for directing the migration of developing spinal neurons towards the ventral spinal cord. Signaling through *Dcc* appears to play an instructive role in ventral migration of early-born neurons. In the absence of *Dcc*, many dI1-3 and dI5 neurons fail to migrate ventrally or ventrolaterally. Intriguingly, some dI5 (*Lmx1b*) neurons even migrate dorsally in $Dcc^{-/-}$ mutants. This suggests that the presence of *Dcc* is sufficient to override the dorsal-driving force exerted by some unknown molecules.

In $Dcc^{-/-}$ mutants, some early-born neurons appear to undergo normal ventral migration. Several factors may account for this observation. First, not all early-born neurons express *Dcc* (Fig. 2). Second, *Dcc* is not the only receptor for netrins, and it may functionally be redundant with other *Dcc* family members such as neogenin genes or Unc5h3 receptors (Ackerman and Knowles, 1998;Engelkamp, 2002;Keino-Masu et al., 1996). Indeed, the observation that a similar defect found in *Unc5h3* mutant mice supports such a possibility (see Fig. S2 in the supplementary material). Thus, multiple receptors for netrins may guide the migration of early-born neurons synergistically. In $Dcc^{-/-}$ mutants, the migration of late-born neurons appears to be normal, despite their proximity to early-born neurons during their migration from the VZ to the superficial dorsal horn, consistent with weak or no expression of *Dcc* in these neurons (see Fig. S1 in the supplementary material). Furthermore, although late-born neurons that take up exogenous *Dcc* fail to settle in the superficial layer of the dorsal horn, other non-electroporated late-born neurons exhibit no apparent aberrant migration. Thus, *Dcc* appears to function in a cell autonomous manner.

The simplest explanation for how *Dcc* controls ventral migration is that it allows early-born neurons to respond to *Ntn1*, which is expressed in the floorplate and perhaps also as a ventral-to-dorsal gradient in the spinal cord (Kennedy et al., 1994). In this aspect, the function of *Dcc* is reminiscent of its role in ventral projection of commissural neurons in the spinal cord (Kennedy et al., 1994). Moreover, that overexpression of *Dcc* in late-born neurons altered their migratory behavior suggests that an intracellular signal transduction pathway that can be activated by *Dcc* may also be present in these neurons.

Our study reveals an unexpected role of early-born neurons in the patterning of primary afferents in the spinal cord. Interestingly, not all early-born neurons are required for the projection of proprioceptive afferents. For example, no obvious defects were found in the projections of proprioceptive afferents in mice lacking *Math1* (Bermingham et al., 2001). In *Lmx1b* mutants, the specification of dI5 neurons is impaired, but proprioceptive afferent do project to the ventral horn (Ding et al., 2004; Gross et al., 2002; Muller et al., 2002). Therefore, at least dI1 and dI5 neurons are dispensable for the projections of proprioceptive afferents.

In $Dcc^{-/-}$ mutants, early-born neurons are mispositioned in the medial superficial dorsal horn to which proprioceptive afferents aberrantly project. This suggests that early-born neurons contain a chemoattractant necessary for directing the projection of proprioceptive afferents. Although *Sema3a* is most notable for its chemorepellent function, it may also function as a chemoattractant in the nervous system (Pasterkamp and Kolodkin, 2003; Polleux et al., 2000). However, the previous finding that *Sema3a* has little influence on NT3-responsive axons raises the possibility that other unknown chemoattractant(s) may be involved (Messersmith et al., 1995). On the other hand, the observation that $TrkA^+$ afferents are excluded from the region where early-born neurons are present argues that early-born neurons have a repulsive function for cutaneous afferents. Several lines of evidence suggest that early-born neurons may exert this function through *Sema3a*. First, *Sema3a* expression is abnormally detected in the region where early-born neurons are ectopically located in the medial superficial dorsal horn (Fig. 8). In addition, forced expression of *Sema3a* in the dorsal horn by in utero electroporation repels $TrkA^+$ primary afferents (Fig. 8). Therefore, our study indicates that *Sema3a* repels cutaneous

afferents in vivo, which is in consistent with studies performed in chicken and rat spinal cord (Fu et al., 2000; Pasterkamp et al., 2000; Shepherd et al., 1997; Tang et al., 2004). It further offers an explanation for why $TrkA^+$ afferents avoid the midline region of the dorsal horn where early-born neurons are present as their entry route. In both chick and mouse spinal cord, the entry of cutaneous primary afferents into the dorsal side of the spinal cord occurs only after a waiting period that is coincident with the abundant presence of early-born neurons and *Sema3a* at the dorsal side of the spinal cord (Shepherd et al., 1997). Thus, a spatial regulated distribution of $Sema3a^+$ in early-born neurons may have a key role in preventing $TrkA^+$ primary afferents from entering the dorsal spinal cord prematurely. Together, our results demonstrate that early-born neurons possess dual roles in guiding the projections of primary afferents: (1) to steer the initial ingrowth of proprioceptive afferents towards the ventral horn; and (2) to repel the nociceptive afferents from the midline region and from the deep dorsal horn.

Our results suggest that an early-born neurons-derived signal is crucial for the initial ingrowth of proprioceptive afferent along the midline and toward the intermediate region within the spinal cord. As *Dcc* is not expressed in DRG neurons, our result is in contrast with previous studies that showed that factors guiding the ventral projection of proprioceptive afferents are most likely to reside in the proprioceptive neurons in the DRG (Arber et al., 2000; Inoue et al., 2002; Lin et al., 1998; Patel et al., 2003). Interestingly, in the absence of *Dcc*, some proprioceptive afferents did manage to project to the intermediate region as well as the ventral horn of the spinal cord at later stages, albeit in much reduced number (Fig. 7). Whether a delay of ventral projection of proprioceptive afferents reflects a partial defect of early-born neurons or a compensation mechanism remains unknown. Nevertheless, because a majority of early-born neurons no longer migrate further once they reach the intermediate region, other signals may come into play for further elongation of those afferents. Together with the findings that transcription factor such as *Er81* and *Runx3* are required in DRG neurons for proprioceptive afferent projection, our data suggest that coordinated signals derived from both primary afferents and their central target neurons within the spinal cord are essential for the projections of the primary afferents.

Acknowledgements

We thank B. Vogelstein, T. Jessell, J. Johnson, L. Recharidt, J. Brunet, P. Labosky, H. Zoghbi, J.-I. Miyazaki, T. Saito and M. Taniguchi for reagents, and J. Johnson and A. Kania for comments on the manuscript. We are grateful for T. Saito's advice on in utero electroporation. We also thank J. Yin and Carl Xiang for technical help. Z.F.C. and Y.R. are supported by NIH (NS43968-01 to Z.F.C. and CA107193 to Y.R.).

References

Ackerman SL, Knowles BB. Cloning and mapping of the UNC5C gene to human chromosome 4q21-q23. Genomics 1998;52:205–208. [PubMed: 9782087]

Arber S, Ladle DR, Lin JH, Frank E, Jessell TM. ETS gene Er81 controls the formation of functional connections between group Ia sensory afferents and motor neurons. Cell 2000;101:485–498. [PubMed: 10850491]

Bermingham NA, Hassan BA, Wang VY, Fernandez M, Banfi S, Bellen HJ, Fritzsch B, Zoghbi HY. Proprioceptor pathway development is dependent on Math1. Neuron 2001;30:411–422. [PubMed: 11395003]

Brown, AG. Organization of the Spinal Cord. The Anatomy and Physiology of Identified Neurons. Berlin: Springer-Verlag; 1981.

Burrill JD, Moran L, Goulding MD, Saueressig H. PAX2 is expressed in multiple spinal cord interneurons, including a population of EN1+ interneurons that require PAX6 for their development. Development 1997;124:4493–4503. [PubMed: 9409667]

Caspary T, Anderson KV. Patterning cell types in the dorsal spinal cord: what the mouse mutants say. Nat Rev Neurosci 2003;4:289–297. [PubMed: 12671645]

Chan SS, Zheng H, Su MW, Wilk R, Killeen MT, Hedgecock EM, Culotti JG. UNC-40, a C. elegans homolog of DCC (Deleted in Colorectal Cancer), is required in motile cells responding to UNC-6 netrin cues. Cell 1996;87:187–195. [PubMed: 8861903]

Chen H, Lun Y, Ovchinnikov D, Kokubo H, Oberg KC, Pepicelli CV, Gan L, Lee B, Johnson RL. Limb and kidney defects in Lmx1b mutant mice suggest an involvement of LMX1B in human nail patella syndrome. Nat Genet 1998a;19:51–55. [PubMed: 9590288]

Chen ZF, Paquette AJ, Anderson DJ. NRSF/REST is required in vivo for repression of multiple neuronal target genes during embryogenesis. Nat Genet 1998b;20:136–142. [PubMed: 9771705]

Chen ZF, Rebelo S, White F, Malmberg AB, Baba H, Lima D, Woolf CJ, Basbaum AI, Anderson DJ. The paired homeodomain protein DRG11 is required for the projection of cutaneous sensory afferent fibers to the dorsal spinal cord. Neuron 2001;31:59–73. [PubMed: 11498051]

Ding YQ, Yin J, Kania A, Zhao ZQ, Johnson RL, Chen ZF. Lmx1b controls the differentiation and migration of the superficial dorsal horn neurons of the spinal cord. Development 2004;131:3693–3703. [PubMed: 15229182]

Dodd J, Morton SB, Karagogeos D, Yamamoto M, Jessell TM. Spatial regulation of axonal glycoprotein expression on subsets of embryonic spinal neurons. Neuron 1988;1:105–116. [PubMed: 3272160]

Engelkamp D. Cloning of three mouse Unc5 genes and their expression patterns at mid-gestation. Mech Dev 2002;118:191–197. [PubMed: 12351186]

Fazeli A, Dickinson SL, Hermiston ML, Tighe RV, Steen RG, Small CG, Stoeckli ET, Keino-Masu K, Masu M, Rayburn H, et al. Phenotype of mice lacking functional Deleted in colorectal cancer (Dcc) gene. Nature 1997;386:796–804. [PubMed: 9126737]

Fearon ER, Cho KR, Nigro JM, Kern SE, Simons JW, Ruppert JM, Hamilton SR, Preisinger AC, Thomas G, Kinzler KW, et al. Identification of a chromosome 18q gene that is altered in colorectal cancers. Science 1990;247:49–56. [PubMed: 2294591]

Finger JH, Bronson RT, Harris B, Johnson K, Przyborski SA, Ackerman SL. The netrin 1 receptors Unc5h3 and Dcc are necessary at multiple choice points for the guidance of corticospinal tract axons. J Neurosci 2002;22:10346–10356. [PubMed: 12451134]

Fu SY, Sharma K, Luo Y, Raper JA, Frank E. SEMA3A regulates developing sensory projections in the chicken spinal cord. J Neurobiol 2000;45:227–236. [PubMed: 11077427]

Gross MK, Dottori M, Goulding M. Lbx1 specifies somatosensory association interneurons in the dorsal spinal cord. Neuron 2002;34:535–549. [PubMed: 12062038]

He Z, Tessier-Lavigne M. Neuropilin is a receptor for the axonal chemorepellent Semaphorin III. Cell 1997;90:739–751. [PubMed: 9288753]

Helms AW, Johnson JE. Progenitors of dorsal commissural interneurons are defined by MATH1 expression. Development 1998;125:919–928. [PubMed: 9449674]

Helms AW, Johnson JE. Specification of dorsal spinal cord interneurons. Curr Opin Neurobiol 2003;13:42–49. [PubMed: 12593981]

Huang EJ, Wilkinson GA, Farinas I, Backus C, Zang K, Wong SL, Reichardt LF. Expression of Trk receptors in the developing mouse trigeminal ganglion: in vivo evidence for NT-3 activation of TrkA and TrkB in addition to TrkC. Development 1999;126:2191–2203. [PubMed: 10207144]

Inoue K, Ozaki S, Shiga T, Ito K, Masuda T, Okado N, Iseda T, Kawaguchi S, Ogawa M, Bae SC, et al. Runx3 controls the axonal projection of proprioceptive dorsal root ganglion neurons. Nat Neurosci 2002;5:946–954. [PubMed: 12352981]

Keino-Masu K, Masu M, Hinck L, Leonardo ED, Chan SS, Culotti JG, Tessier-Lavigne M. Deleted in colorectal cancer (DCC) encodes a netrin receptor. Cell 1996;87:175–185. [PubMed: 8861902]

Kennedy TE, Serafini T, de la Torre JR, Tessier-Lavigne M. Netrins are diffusible chemotropic factors for commissural axons in the embryonic spinal cord. Cell 1994;78:425–435. [PubMed: 8062385]

Kolodkin AL, Levengood DV, Rowe EG, Tai YT, Giger RJ, Ginty DD. Neuropilin is a semaphorin III receptor. Cell 1997;90:753–762. [PubMed: 9288754]

Lee KJ, Jessell TM. The specification of dorsal cell fates in the vertebrate central nervous system. Annu Rev Neurosci 1999;22:261–294. [PubMed: 10202540]

Lee KJ, Mendelsohn M, Jessell TM. Neuronal patterning by BMPs: a requirement for GDF7 in the generation of a discrete class of commissural interneurons in the mouse spinal cord. Genes Dev 1998;12:3394–3407. [PubMed: 9808626]

Lee KJ, Dietrich P, Jessell TM. Genetic ablation reveals that the roof plate is essential for dorsal interneuron specification. Nature 2000;403:734–740. [PubMed: 10693795]

Lin JH, Saito T, Anderson DJ, Lance-Jones C, Jessell TM, Arber S. Functionally related motor neuron pool and muscle sensory afferent subtypes defined by coordinate ETS gene expression. Cell 1998;95:393–407. [PubMed: 9814709]

Luo Y, Raible D, Raper JA. Collapsin: a protein in brain that induces the collapse and paralysis of neuronal growth cones. Cell 1993;75:217–227. [PubMed: 8402908]

Messersmith EK, Leonardo ED, Shatz CJ, Tessier-Lavigne M, Goodman CS, Kolodkin AL. Semaphorin III can function as a selective chemorepellent to pattern sensory projections in the spinal cord. Neuron 1995;14:949–959. [PubMed: 7748562]

Muller T, Brohmann H, Pierani A, Heppenstall PA, Lewin GR, Jessell TM, Birchmeier C. The homeodomain factor lbx1 distinguishes two major programs of neuronal differentiation in the dorsal spinal cord. Neuron 2002;34:551–562. [PubMed: 12062039]

Murase S, Horwitz AF. Deleted in colorectal carcinoma and differentially expressed integrins mediate the directional migration of neural precursors in the rostral migratory stream. J Neurosci 2002;22:3568–3579. [PubMed: 11978833]

Niwa H, Yamamura K, Miyazaki J. Efficient selection for high-expression transfectants with a novel eukaryotic vector. Gene 1991;108:193–199. [PubMed: 1660837]

Ozaki S, Snider WD. Initial trajectories of sensory axons toward laminar targets in the developing mouse spinal cord. J Comp Neurol 1997;380:215–229. [PubMed: 9100133]

Pasterkamp RJ, Kolodkin AL. Semaphorin junction: making tracks toward neural connectivity. Curr Opin Neurobiol 2003;13:79–89. [PubMed: 12593985]

Pasterkamp RJ, Giger RJ, Baker RE, Hermens WT, Verhaagen J. Ectopic adenoviral vector-directed expression of Sema3A in organotypic spinal cord explants inhibits growth of primary sensory afferents. Dev Biol 2000;220:129–141. [PubMed: 10753505]

Patel TD, Kramer I, Kucera J, Niederkofler V, Jessell TM, Arber S, Snider WD. Peripheral NT3 signaling is required for ETS protein expression and central patterning of proprioceptive sensory afferents. Neuron 2003;38:403–416. [PubMed: 12741988]

Polleux F, Morrow T, Ghosh A. Semaphorin 3A is a chemoattractant for cortical apical dendrites. Nature 2000;404:567–573. [PubMed: 10766232]

Qian Y, Shirasawa S, Chen CL, Cheng L, Ma Q. Proper development of relay somatic sensory neurons and D2/D4 interneurons requires homeobox genes Rnx/Tlx-3 and Tlx-1. Genes Dev 2002;16:1220–1233. [PubMed: 12023301]

Roberts CW, Shutter JR, Korsmeyer SJ. Hox11 controls the genesis of the spleen. Nature 1994;368:747–749. [PubMed: 7908720]

Saba R, Nakatsuji N, Saito T. Mammalian BarH1 confers commissural neuron identity on dorsal cells in the spinal cord. J Neurosci 2003;23:1987–1991. [PubMed: 12657654]

Saito T, Nakatsuji N. Efficient gene transfer into the embryonic mouse brain using in vivo electroporation. Dev Biol 2001;240:237–246. [PubMed: 11784059]

Schwarting GA, Kostek C, Bless EP, Ahmad N, Tobet SA. Deleted in colorectal cancer (DCC) regulates the migration of luteinizing hormone-releasing hormone neurons to the basal forebrain. J Neurosci 2001;21:911–919. [PubMed: 11157077]

Shepherd IT, Luo Y, Lefcort F, Reichardt LF, Raper JA. A sensory axon repellent secreted from ventral spinal cord explants is neutralized by antibodies raised against collapsin-1. Development 1997;124:1377–1385. [PubMed: 9118808]

Tang XQ, Tanelian DL, Smith GM. Semaphorin3A inhibits nerve growth factor-induced sprouting of nociceptive afferents in adult rat spinal cord. J Neurosci 2004;24:819–827. [PubMed: 14749426]

Wang HU, Chen ZF, Anderson DJ. Molecular distinction and angiogenic interaction between embryonic arteries and veins revealed by ephrin-B2 and its receptor Eph-B4. Cell 1998;93:741–753. [PubMed: 9630219]

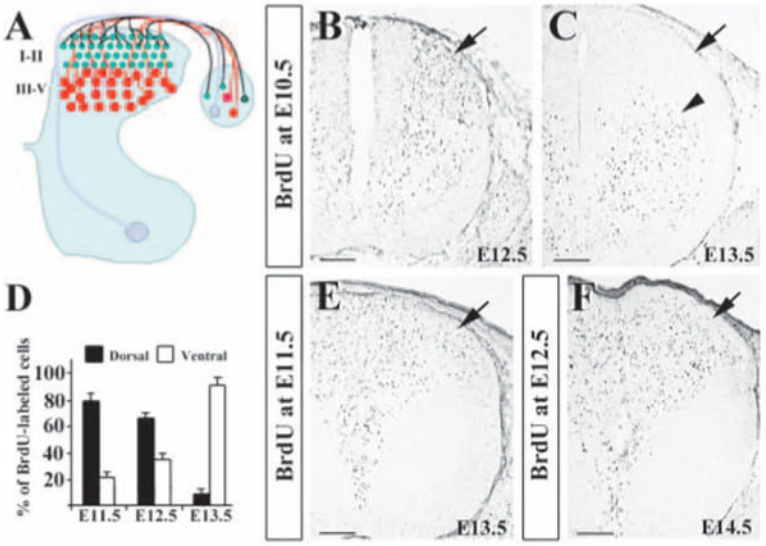

Fig. 1.

Organization of the dorsal horn circuitry and identification of two waves of neuronal migration in the dorsal spinal cord by BrdU labeling. (A) Schematic diagram of the spinal cord circuitry. The dorsal horn can be divided into several laminae. Laminae I-II (green) consist of small neurons in the superficial dorsal horn, whereas laminae III-V (red) contain large neurons in the deep dorsal horn. Proprioceptive afferents (light pink) innervate the motoneurons in the ventral horn via a medial entry route. In the dorsal horn, while mechanoreceptive afferents (red) project to laminae III-IV, nociceptive afferents (green) project mainly to laminae I-II. (B,C) Distribution of E10.5 BrdU-labeled cells in E12.5 (B) and E13.5 (C) dorsal horns. There are no BrdU-labeled cells in the superficial layer of E13.5 dorsal horns (arrow in C). (D) Quantitative comparisons of E10.5 BrdU-labeled cells between the dorsal and ventral horn at E11.5, E12.5 and E13.5. The percentages of BrdU-labeled cells in the dorsal half of the spinal cord (black bar) decreases (79.5%, 62.7% and 9.4%) progressively, while those of the labeled cells in the ventral half (white bar) increases accordingly. (E) E11.5 BrdU-labeled cells in E13.5 spinal cord. (F) E12.5 BrdU-labeled cells in E14.5 spinal cord. Scale bars: 100 μm in B-D,F.

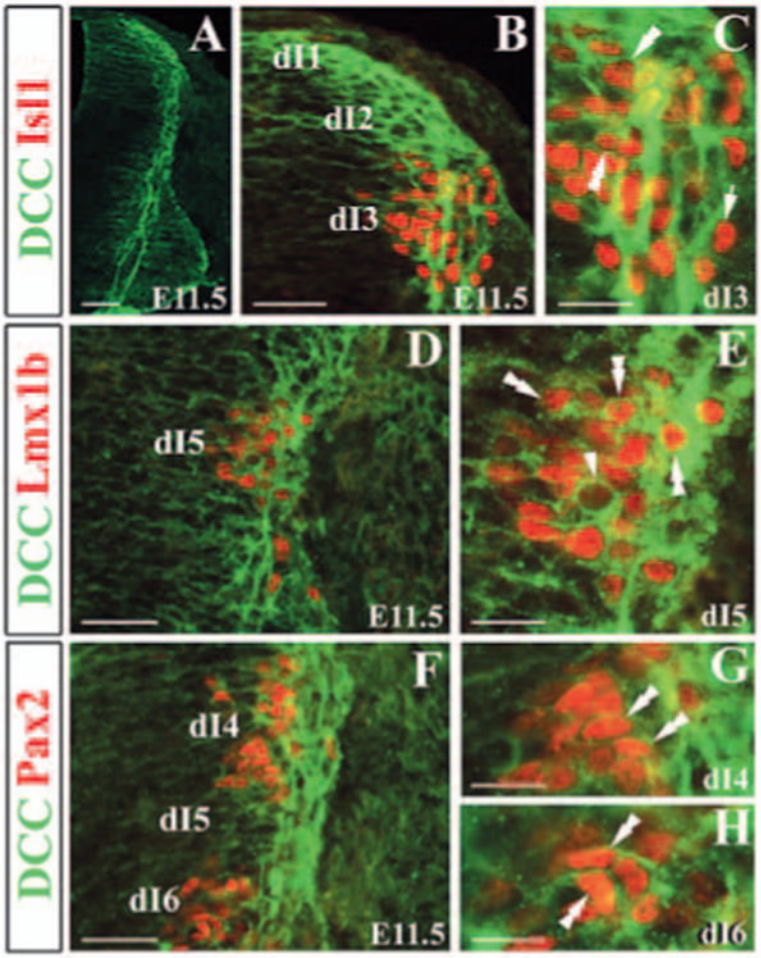

Fig. 2.

Expression of *Dcc* in early-born dorsal interneurons. (A) Immunocytochemical staining of *Dcc* of E11.5 neural tube shows *Dcc* expression in the region lining the VZ of the neural tube. (B) Double immunocytochemical staining of *Dcc* (green) and *Isl1* (red) in E11.5 dorsal spinal cord shows *Isl1* in the nuclei and *Dcc* on membrane and in axons. (C) Higher magnification of B. Some $Isl1^{+}$ cells were not stained for *Dcc* (arrow in C). (D) Double staining of *Dcc* (green) and *Lmx1b* (red). (E) Higher magnification of (D). Some Dcc^{+} cells do not express *Lmx1b* (arrowhead in E). (F) Double staining of *Dcc* (green) and *Pax2* (red; dI4 and dI6 marker). (G) Higher magnification of dI4 region. (H) Higher magnification of dI6 region. Double arrowheads indicate double labeled-neurons. Scale bars: 100 μm in A; 50 μm in B,D,F; 25 μm C,E,G,H.

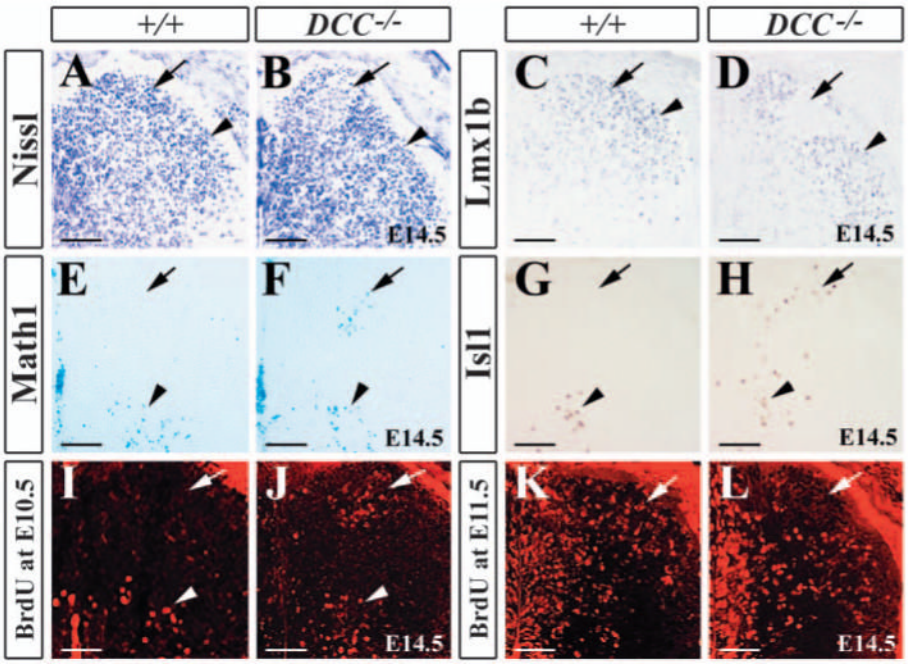

Fig. 3.

Impaired ventral migration of early-born neurons in *Dcc*$^{-/-}$ mutants. (A,B) Nissl staining of the dorsal horn of wild-type embryo (A) and DCC$^{-/-}$ mutant (B) embryos. Arrow in (B) indicates an area that is lightly stained with Nissl in the medial part of laminae I-II. (C,D) Immunocytochemical staining of *Lmx1b* in the dorsal horn of wild-type (C) and *Dcc*$^{-/-}$ mutant (D) embryos shows *Lmx1b*$^{+}$ neurons in laminae I-II (arrow and arrowhead in C) and the region lacking *Lmx1b* staining (arrow in D). (E,F) X-gal staining of E14.5 *Math1*$^{+/-}$ (E) and *Math1*$^{+/-}$/*Dcc*$^{-/-}$ embryos (F) shows an absence of *Math1*$^{+}$ cells in the dorsal horn (arrow) of *Math1*$^{+/-}$ embryos in contrast to the ectopic *Math1*$^{+}$ cells in the medial superficial dorsal horn in *Dcc*$^{-/-}$ mutants (arrow in F). Arrowheads indicate *Math1*$^{+}$ cells in the intermediate region of the spinal cord. (G,H) *Isl1* staining of wild-type (G) and *Dcc*$^{-/-}$ mutant (H) embryos shows the ectopic *Isl1*$^{+}$ cells in the dorsal horn of *Dcc*$^{-/-}$ mutants (arrow in H) when compared with wild-type control. Arrowheads indicate *Isl1*$^{+}$ cells in the intermediate region of the spinal cord. (I,J) E10.5 BrdU-labeled neurons are detected in the dorsal half of the spinal cord of wild-type (I) and *Dcc*$^{-/-}$ mutant (J) embryos at E14.5. Arrows indicate a cluster of BrdU-labeled neurons in the medial superficial dorsal horn of the mutant (J), but not in wild-type (I). Arrowheads indicate BrdU-labeled neurons at the intermediate region of wild-type and *Dcc*$^{-/-}$ mutant embryos. (K,L). E11.5 BrdU-labeled neurons are seen in the dorsal horn of wild-type (K) and *Dcc*$^{-/-}$ mutant (L) embryos. Arrows indicate an absence of BrdU-labeled neurons in the medial superficial dorsal horn of the mutants. Scale bars: 100 μm.

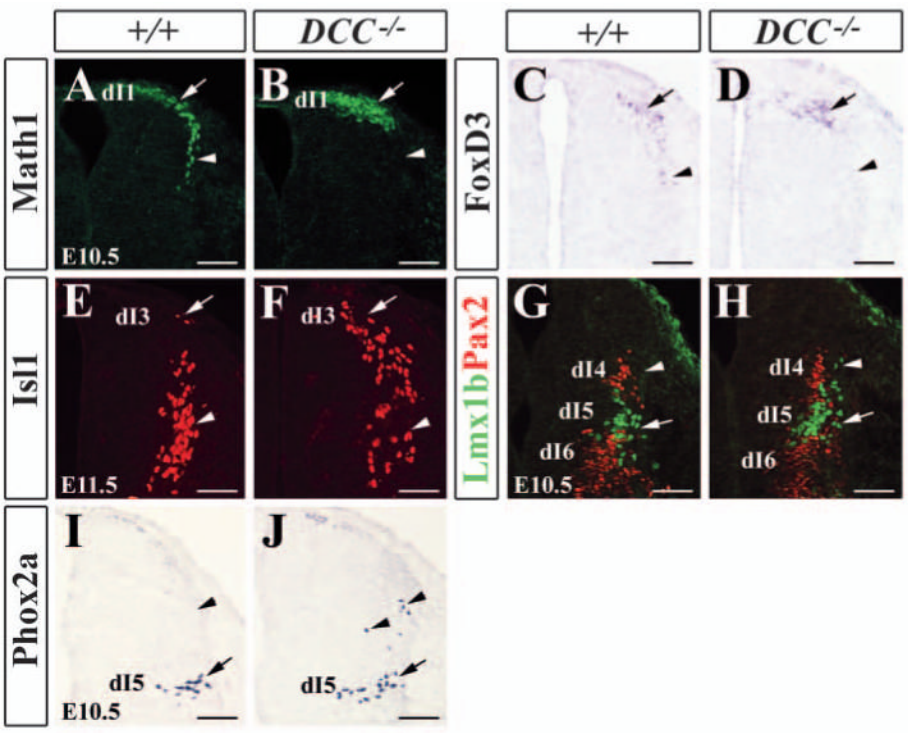

Fig. 4.

Expression of early-born neuron-specific markers in wild-type and $Dcc^{-/-}$ mutants. (A,B) *Math1* immunocytochemical staining of E10.5 wild-type (A) and $Dcc^{-/-}$ mutant (B) dorsal neural tubes shows an absence of $Math1^{+}$ cells in more ventral aspect of the neural tube of $Dcc^{-/-}$ mutant (arrowhead in B) when compared with wild-type control (arrowhead in A). (C,D) *Foxd3* (dI2 marker) expression in E10.5 wild-type (C) and $Dcc^{-/-}$ mutant (D) neural tubes detected by in situ hybridization. $Foxd3^{+}$ cells are absent in more ventral aspect of the neural tube, as indicated by arrowhead in D. (E,F) *Isl1* staining of E11.5 wild-type (E) and $Dcc^{-/-}$ mutant (F) neural tubes. More $Isl1^{+}$ cells are present in the dorsal part of the neural tube (arrow in F). (G,H) Double staining of *Lmx1b* (green; dI5 marker) and *Pax2* (red; dI4, dI6 marker) in E10.5 wild-type (G) and $Dcc^{-/-}$ mutant (H) neural tubes. Arrowhead in H indicates dorsally migrated $Lmx1b^{+}$ cells. (I,J) *Phox2a* staining of E10.5 wild-type (I) and $Dcc^{-/-}$ mutant (J) neural tubes. Arrows and arrowheads in I,J indicate normal and abnormal positions of $Phox2a^{+}$ neurons, respectively. Scale bars: 100 μm.

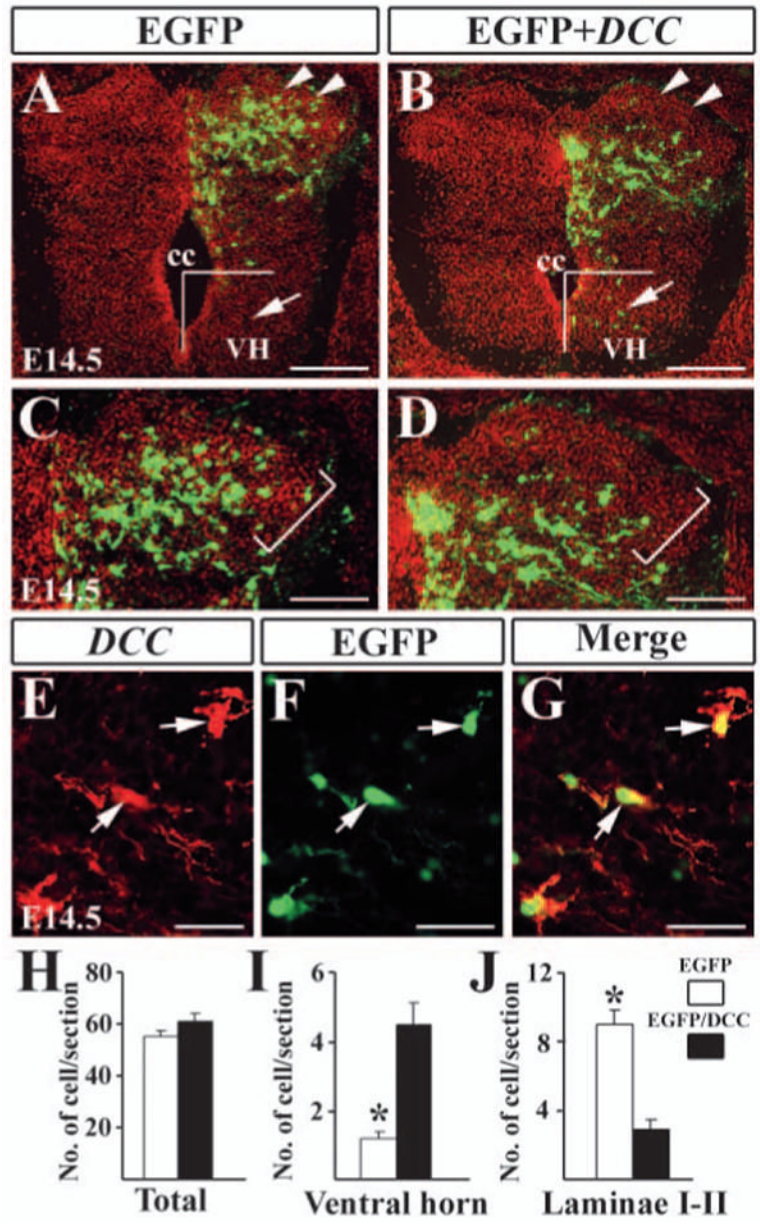

Fig. 5.

Forced expression of *Dcc* in the dorsal spinal cord. (A,B) Detection of EGFP in the dorsal spinal cord electroporated with EGFP only (A) and *Egfp/Dcc* (B) plasmids. There are a few neurons located in the ventral horn of the spinal cord after the electroporation of *Egfp/Dcc* (arrowheads in B). (C,D) Higher magnification of A,B indicates the superficial dorsal horn. Brackets outline laminae I-II region. In the spinal cord electroporated with EGFP, $EGFP^+$ cells are found in laminae I-II, but few $Egfp/Dcc^+$ cells are present in the corresponding region (D). (E) *Dcc* immunostaining of *Egfp/Dcc* electroporated side of the dorsal horn. Arrows indicate Dcc^+ neurons in the same region. (F) Arrows indicate $EGFP^+$ neurons. (G) *Dcc* and *Egfp* are colocalized in the same cells (arrows). (H-J) Counting of $EGFP^+$ and $Egfp/Dcc^+$ cells in the spinal cord (H), ventral horn (I) and laminae I-II (J). For cell counting in the ventral horn, $Egfp/Dcc^+$ or $EGFP^+$ cells located ventral to the center of the central canal were included, as shown in A,B. For cell counting in laminae I-II, the morphology of the spinal cord is revealed by

Hoechst counterstaining (red color in A-D), and labeled cells in laminae I-II, as shown in C,D were counted. Student's *t*-test was used when making comparisons, **P*<0.0001. cc, central canal; VH, ventral horn. Scale bars: 200 μm in A,B; 100 μm in C,D; 25 μm in E-G.

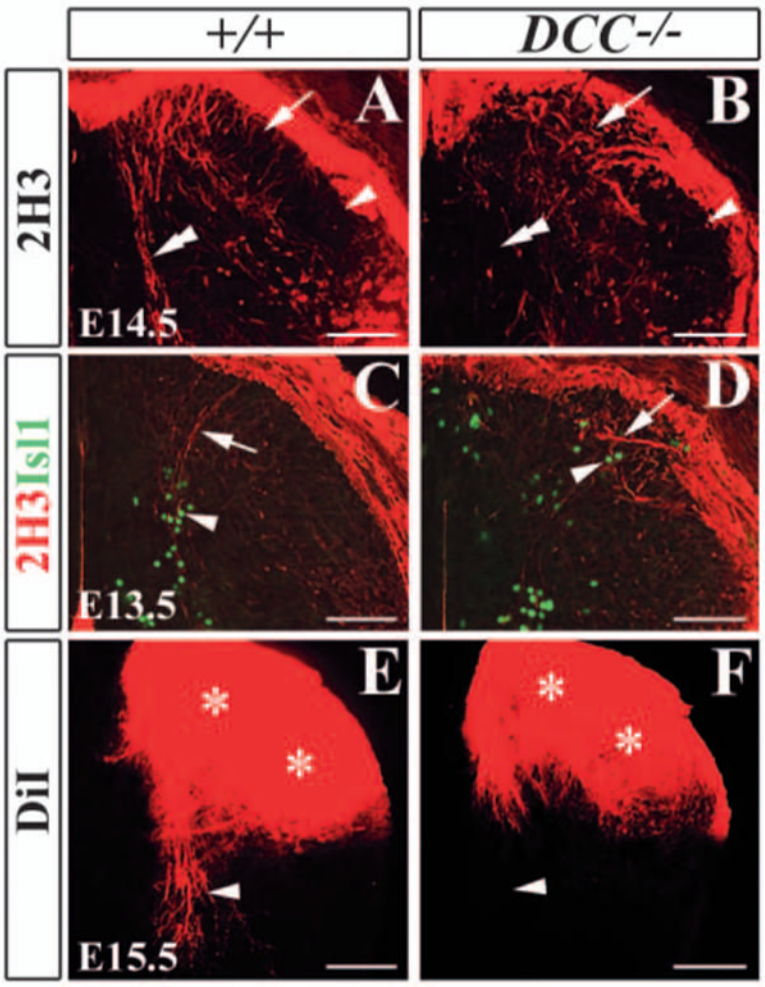

Fig. 6.

Abnormal projection of proprioceptive afferents in *Dcc*$^{-/-}$ mutants. (A,B) 2H3 immunocytochemical staining indicates an absence of 2H3^{+} afferent projections to the ventral horn in E14.5 *Dcc*$^{-/-}$ mutant spinal cord (B) when compared with wild-type control (A) (double arrowheads in A,B). 2H3^{+} afferents are aberrantly located in the medial superficial dorsal horn of *Dcc*$^{-/-}$ mutant (arrows in B). (C,D) Double immunocytochemical staining of 2H3 and *Isl1* in E13.5 wild-type (C) and *Dcc*$^{-/-}$ mutant (D) dorsal horns shows that 2H3^{+} afferents (arrows in C,D) appear to follow the pattern of *Isl1*$^{+}$ staining (arrowheads in C,D). (E,F) DiI labeling of E15.5 wild-type (E) and *Dcc*$^{-/-}$ mutant (F) spinal cords shows no proprioceptive afferents growing towards the ventral horn in *Dcc*$^{-/-}$ mutant (arrowheads in E,F). Asterisks indicate the heavily labeled superficial dorsal horn by DiI. Scale bars: 100 μm.

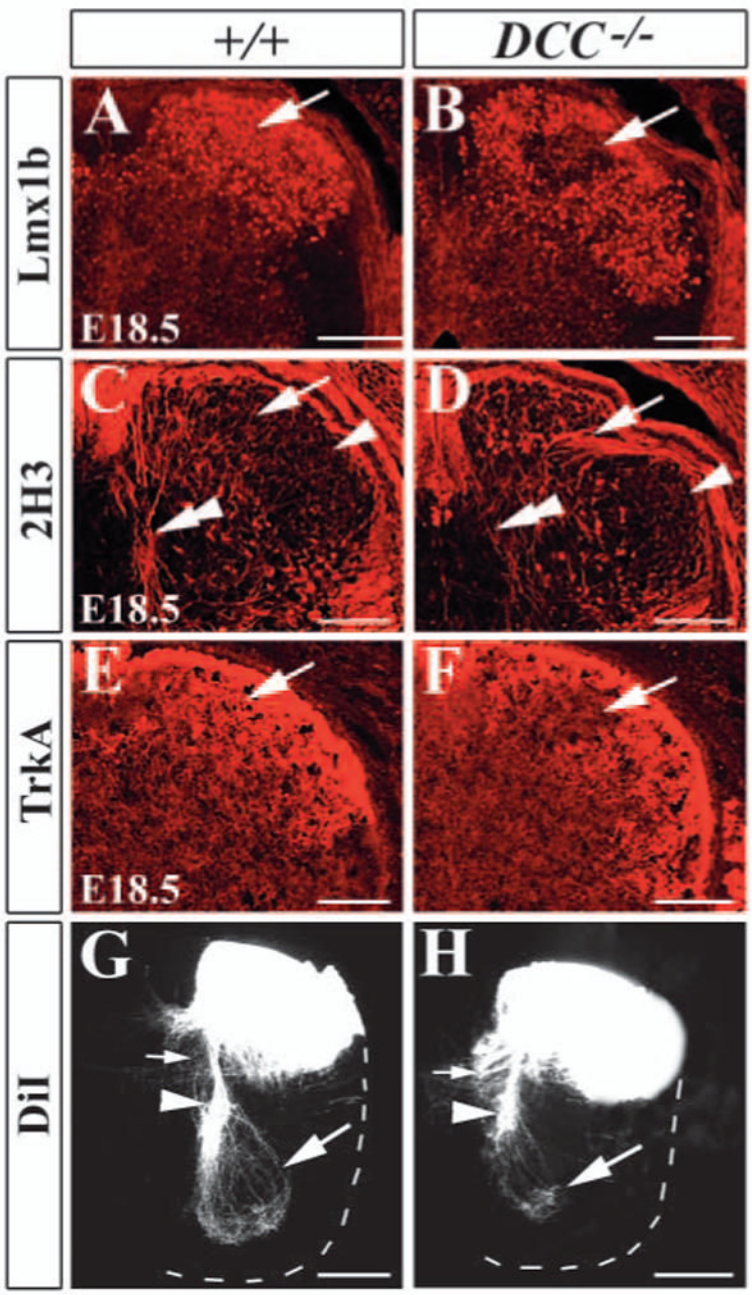

Fig. 7.

Abnormal projection of proprioceptive afferents in *Dcc*$^{-/-}$ mutants at E18.5. (A,B) Immunocytochemical staining of *Lmx1b* shows the distribution of *Lmx1b*$^{+}$ neurons in the superficial dorsal horn of the wild-type mice (A), and the region lacking *Lmx1b*$^{+}$ neurons (arrow in B) in the dorsal horn of *Dcc*$^{-/-}$ mutants at E18.5. (C,D) 2H3 staining shows the absence of 2H3^{+} primary afferents to the ventral horn (double arrowhead in D) and its abnormal location in the superficial dorsal horn (arrow in D) in *Dcc*$^{-/-}$ mutants (D), compared with wild-type mice (C). (E,F) TrkA immunostaining shows the absence of TrkA^{+} primary afferent in the medial superficial dorsal horn in *Dcc*$^{-/-}$ mutants (arrow in F). In wild-type mice, TrkA^{+} fibers are evenly distributed in the superficial dorsal horn (E). (G,H) DiI labeling shows a dramatic reduction of proprioceptive projection to the ventral horn (large arrow in H) and

abnormal projection to the midline region (small arrow in H) of *Dcc*$^{-/-}$ mutant, compared with wild-type mice (G). Broken white lines outline the ventral horn of the spinal cord. Scale bars: 100 μm.

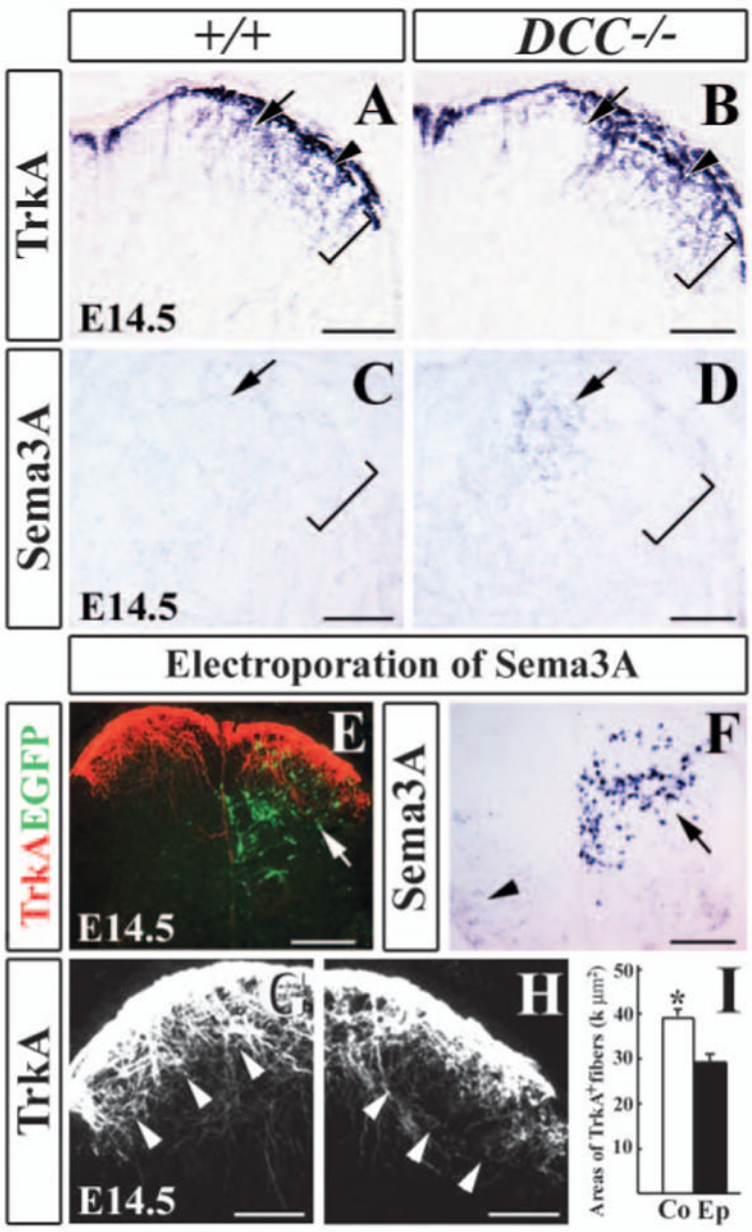

Fig. 8.

Early-born neurons and *Sema3a* repel TrkA^{+} afferents in the dorsal spinal cord. (A,B) TrkA immunocytochemical staining of E14.5 wild-type (A) and *Dcc*$^{-/-}$ mutant (B) spinal cords shows an absence of TrkA $^{+}$ afferents in the medial superficial dorsal horn of *Dcc*$^{-/-}$ mutant (arrow in B) when compared with wild-type control (arrow in A). Brackets in A-D indicate superficial dorsal horn. (C,D) In situ hybridization in wild-type (C) and *Dcc*$^{-/-}$ mutant (D) dorsal horn shows the ectopic *Sema3a* in the medial superficial dorsal horn of the mutant (arrow in D) when compared with wild-type control (arrow in C). (E) Immunocytochemical staining of TrkA^{+} afferents (red) and EGFP (green; arrow in E) in *Sema3a*+EGFP co-electroporated spinal cord. (F) Strong *Sema3a* expression in electroporated spinal dorsal horn. Arrow indicates introduced *Sema3a* expression, whereas arrowhead indicates endogenous *Sema3a* expression in the ventral horn. (G,H) Higher magnifications of E, showing TrkA staining of the contralateral (G) and electroporated sides (H) of the spinal cord. On the contralateral side of

the dorsal horn, strong TrkA staining is detected in laminae I-II (arrowheads in G), but on the electroporated side much less TrkA staining is seen in laminae I-II (arrowheads in H). (I) Quantitative analysis of TrkA-positive areas. Asterisk indicates a significant difference in the area of TrkA-positive staining. **P*<0.001. Areas of $TrkA^+$ fibers are expressed by k μm^2; k=1000. Co, contralateral side; Ep, electroporated side. Scale bars: 200 μm in E,F; 100 μm in A-D,G,H.